

Controlled synthesis and optical transmission characteristics of silicon nanowires on colloid patterned glass substrates

Dong Hyun Lee, Yong Bum Pyun, Kwang-Soo Son, Jae-Woong Choung, Jung-Min Lee, Seong Jun Son and Won Il Park*

Division of Materials Science and Engineering, Hanyang University, Seoul 133-791, Korea

We report the patterned synthesis of silicon nanowire (SiNW) arrays by controlling the density and position of Au colloids on glass substrates in a nanocolloid-catalyzed chemical vapor deposition (CVD) process. Density-controlled colloidal Au patterns were defined on the substrates by an inverse contact imprinting technique, where the strong attractive force between electrolyte-coated polymer stamp surfaces and Au colloids was exploited for selective removal of Au colloids from contacting regions of the substrate to the stamp. Controlled nanocolloid-catalyzed CVD process led to the growth of SiNWs being rooted in the catalytic patterns and extended over several tens of μm . In addition, optical transmittance of the SiNW pattern arrays depending on the NW density and the coverage of catalytic patterns were investigated to understand the optical properties of SiNW arrays.

Key words: Silicon nanowires, Selective growth, Contact imprinting, Optical transmittance.

Introduction

Many semiconductor devices in the emerging electronic and optoelectronic systems demand novel material systems exhibiting new mechanical and optical functions plus their intrinsic properties [1, 2]. For example, next-generation foldable devices require the development of mechanically flexible semiconductor materials that can be deposited on large-scale plastics substrates [3]. For these applications, one-dimensional (1D) inorganic nanomaterials, such as silicon nanowires (SiNWs), would be suitable candidates since the 1D nanostructures provide a significant enhancement in mechanical flexibility, while their single-crystalline structures hold the promise of high device performance, comparable to conventional semiconductor devices [4-6]. On the other hand, numerical analysis based on effective-medium model predicts that periodic SiNW arrays suspended in air have much lower reflectivity than thin films, revealing an increase in absorption and/or transmittance of incident light in SiNWs [7]. The antireflection effect represents the potential use of SiNWs in transparent electronics and photovoltaic devices [7-9]. However, two such devices require the contradictory criteria; high optical transmittance in the visible spectral range should be preferred over optical absorption in transparent electronic applications [10-13], whereas the efficiency of a solar cell is determined by optical absorption in the solar spectral range. Understanding optical processes

in SiNWs is therefore crucially important to design SiNW optoelectronic systems to be suitable for their applications.

On the other hand, optical processes as well as charge carrier transport in SiNW arrays are strongly affected by NW size, density, and arrangement. It would be therefore desirable to find a synthetic strategy to grow SiNWs in a controllable manner for both scientific studies and practical device applications [14, 15]. In this paper, by combining a nanocolloid-catalyzed chemical vapor deposition (CVD) process, and a colloid patterning technique, selective and lateral growth of SiNW arrays on glass substrates is demonstrated. In addition, to understand the optical properties of SiNWs and to find the optimal design of SiNW patterns for electronic and optoelectronic applications, we studied the correlation between optical transmittance in the SiNW arrays and colloidal Au patterns that determine the density and size of SiNWs.

Experimental

For selective and lateral growth of SiNWs, Au colloids were patterned on glass substrates via an inverse contact imprinting (ICI) process. First, to deposit the negatively charged Au colloids on glass substrates, the substrate surfaces were coated with positively charged poly-L-lysine, followed by rinsing with deionized water (Fig. 1(a)) [16, 17]. After drying in a nitrogen flow, the glass substrates were immersed in a 20-nm-diameter colloidal Au solution for 5 minutes (Fig. 1(b)). The density of Au colloid on the substrates was controlled by diluting the colloidal Au solutions to $\sim 2 \times 10^9$ particles/ml, $\sim 4 \times 10^9$ particles/ml, and $\sim 2 \times 10^{10}$ particles/ml with H_2O . Second, colloidal Au patterns were defined by selective

*Corresponding author:
Tel : +82-2-2220-0504
Fax: +82-2-2220-0387
E-mail: wipark@hanyang.ac.kr

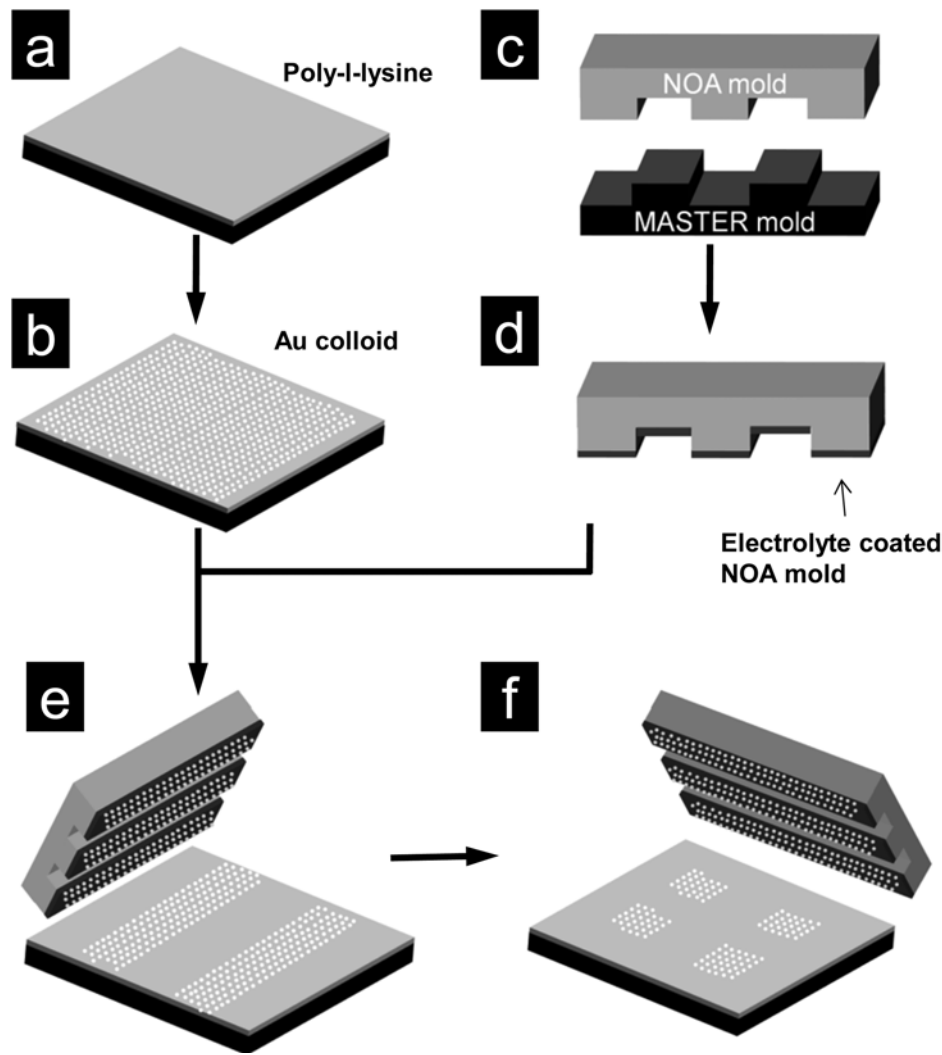


Fig. 1. Schematic illustrating the method used for Au colloid patterning by the ICI process. (a-b) Preparation of Au colloid coated glass substrate; the substrate is coated with positively charged poly-L-lysine (a), and then immersed in a colloidal Au solution for 5 minutes (b), (c-d) Preparation of NOR stamp; NOR stamp is made by using a Si master mold (c), and then coated with the electrolyte (d), (e) Preparation of the line patterns of the Au colloids; the NOR stamp is placed on the glass substrates coated with Au colloids, followed by pressing at a pressure of ~ 350 g/cm² and heating at 80 °C for 10 minutes, (f) Preparation of the colloidal Au square patterns by a second ICI in a perpendicular direction to the line patterns.

removal of Au colloids from contacting regions of the substrate to a polymer stamp. To prepare the polymer stamp, an ultraviolet (UV) curable polymer, Norland Optical Adhesive (NOR) 63, was cast on a Si master mold (with 20-40 μ m line/separation), and then cured with UV light (Fig. 1(c)) [18]. The NOR stamp surface was coated with electrolyte, and then placed on the glass substrates coated with Au colloids (Fig. 1(d)), followed by pressing at a pressure of ~ 350 g/cm² and heating at 80 °C for 10 minutes. Due to the strong attractive force between the electrolyte-coated NOR stamp surfaces and Au colloids, most of the Au colloids in the contacting regions of the substrate/stamp surface were transferred to the stamp, producing 1D arrays of Au colloid line patterns (Fig. 1(e)). In addition, 2D square patterns of Au colloids can also be prepared by a second ICI process in a perpendicular direction to the original line patterns (Fig. 1(f)).

The colloid patterned substrates prepared in this way were then transferred to the CVD chamber for selective growth of SiNWs. During SiNW growth, H₂ and SiH₄ (10% diluted in H₂) flow rates were controlled in the range of 10-30 sccm and 30-100 sccm, respectively. The reactor pressure and temperature were kept at 40 torr (5.3 kPa) and 520 °C, respectively, and the typical growth time was 15 minutes.

Results and Discussion

Fig. 2 shows the optical microscopy (OM) and the atomic force microscopy (AFM) images of Au colloid patterns with 40 μ m lines and 40 μ m separation that have been prepared with a colloidal Au solution diluted to $\sim 4 \times 10^9$ particles/ml. The density of the Au colloid deposited inside the line patterns is ~ 200 -250 particles/ μ m² (Fig. 2(b)), which is comparable to that on the substrate

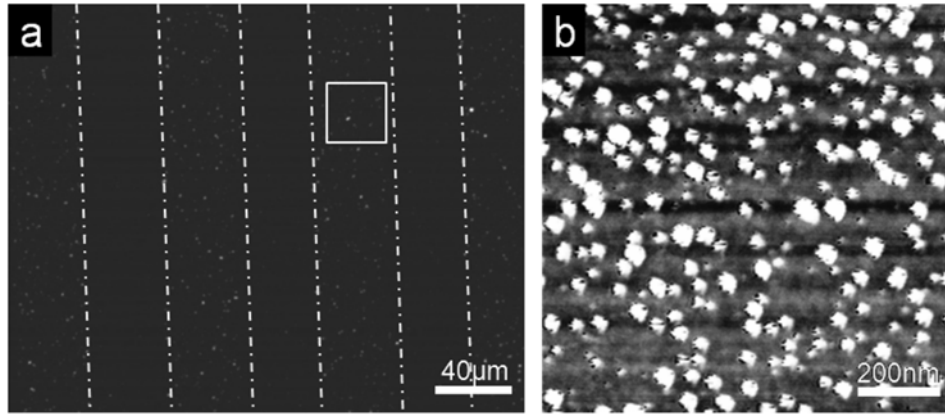


Fig. 2. (a) OM image of the colloidal Au patterns with 40 μm lines and 40 μm separation formed by the ICI process. (b) AFM image of Au colloids deposited inside the line patterns.

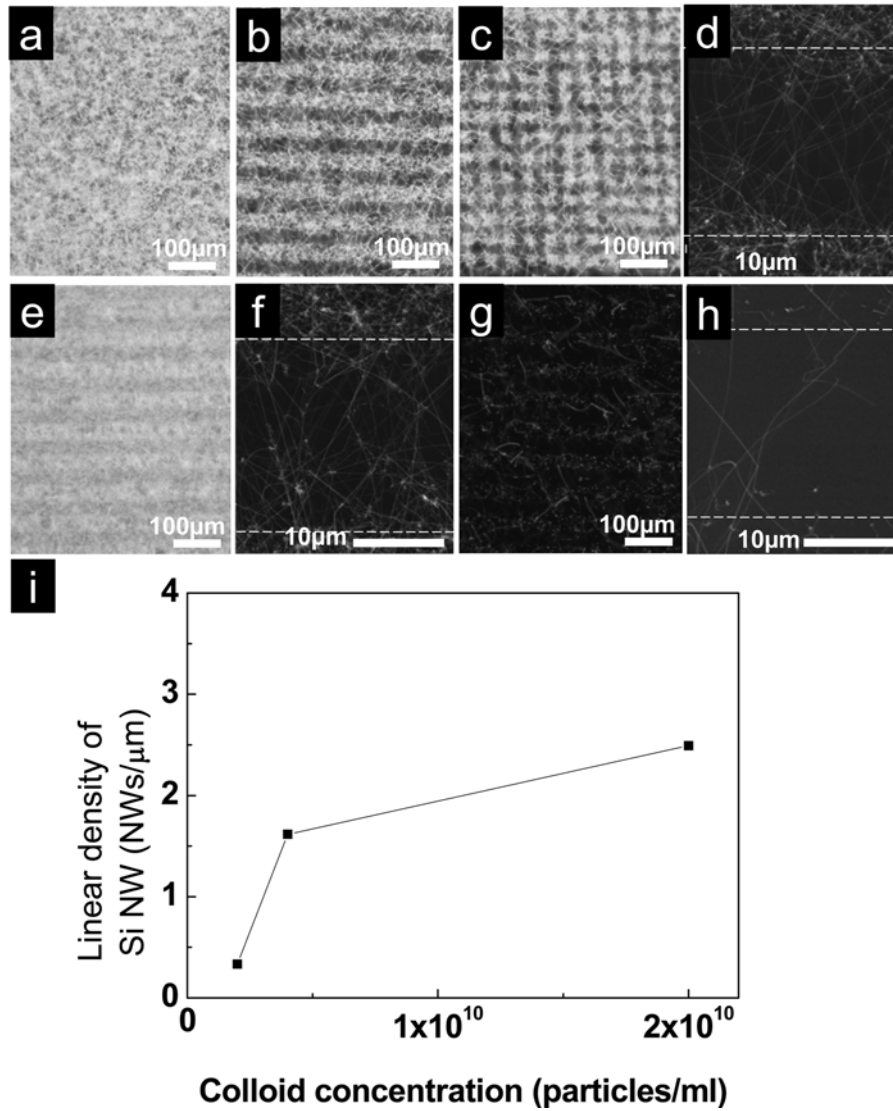


Fig. 3. (a-c) OM image of SiNWs produced from 20-nm-diam Au colloids deposited on the substrate with a colloidal Au solution diluted to $\sim 4 \times 10^9$ particles/ml without (a) and with ICI processes (b, c), (b) SiNWs selectively grown on the colloidal line patterns with 40 μm lines and 40 μm separation, (c) SiNWs selectively grown on the colloidal square patterns with 20 μm width and 40 μm height, (d) SEM image of SiNWs in (c), (e-h) OM and SEM images of SiNWs produced from colloidal patterns prepared with different colloidal Au solutions dilutions to $\sim 2 \times 10^{10}$ particles/ml (e, f) and $\sim 2 \times 10^9$ particles/ml (g, h). The dashed lines in the SEM images (d, f, h) indicate the edges of catalytic patterns, (i) Plot of average linear density of SiNWs measured outside the catalytic patterns versus concentration of the colloidal Au solution.

immediately after the Au colloid deposition. In contrast, a very low density of Au colloids (below ~ 1 particle/ μm^2) remains outside the patterns. This result indicates that most of the Au colloids are transferred from contacting regions of the substrate to the electrolyte-coated NOR stamp that has a higher attractive force to the Au colloids than the substrate.

After preparing the patterned substrates, SiNWs are grown by a nanocolloid-catalyzed vapor-liquid-solid process in the CVD system, where Au nanocolloids define the nucleation and elongation of NWs [19,20]. It is therefore predicted that the diameter, density, and location of SiNWs are strongly affected by those of the Au colloids. Figs. 3(a)–(c) show the OM images of the SiNWs produced from 20-nm-diam Au colloids ($\sim 4 \times 10^9$ particles/ml) without (a) and with ICI processes (b, c). In comparison to SiNWs produced from the Au colloids dispersed on the entire substrate surface (Fig. 3(a)), we found that growth of SiNWs from the stripe or square patterns of Au colloids led to patterned growth of SiNWs (Figs. 3(b) and (c)). A field-emission scanning electron microscopy (FE-SEM) image more clearly shows that very thin SiNWs are rooted in the catalytic patterns and laterally aligned (Fig. 3(d)). It is noted that most of the SiNWs extend over several tens of μm , and are bridging adjacent patterns [20].

In addition, the density of SiNWs grown from the patterns could be controlled by varying the density of the Au colloid in the patterns. Figs. 3(e) and (g) show the SiNWs grown from the square patterns (20 μm in width and 40 μm in height), where the density of the Au colloid was tuned by using different concentration of the colloidal Au solution in the range of $\sim 2 \times 10^9$ – 2×10^{10} particles/ml. The linear density of SiNWs coming off the patterns were determined from the SEM images (Figs. 3(d), (f) and (h)), and the correlation between the nanowire density and the concentration of the colloidal Au solution is summarized in Fig. 3(i).

The ability to grow SiNW pattern arrays on glass substrates with controlled densities can provide an opportunity to study the optical properties of SiNWs.

Optical transmittance spectra of SiNWs produced from the Au colloids deposited on entire glass substrates (Fig. 4(a)) and from the catalytic patterns with 40 μm line/spacing (Fig. 4(b)), show several important points. First, both of these cases present a strong dependence of optical transmittance on the spectral wave length; very opaque to incident short-wavelength light with wavelengths below ~ 400 nm while relatively transparent in the long-wavelength spectral region of 700–800 nm. At a wavelength of 800 nm, SiNWs with a linear density of 0.33 NWs/ μm produced from colloidal Au patterns have transmittances of 81% (Fig. 4(b)). Second, reducing the coverage of Au colloids to 50% of the substrates resulted in nearly double the transmittance in the whole spectra region from 300 nm to 800 nm. The transmittance is also affected by the density of SiNWs that have been controlled by varying the concentration of the colloidal Au solutions. Meanwhile, even though the linear densities of SiNWs were increased by ~ 5 times (from 0.33 NWs/ μm to 1.6 NWs/ μm) and ~ 7 times (from 0.33 NWs/ μm to 2.4 NWs/ μm), the optical transmittance are decreased just 1.3 and 2.23 times, respectively. Our observations demonstrate that the transmittance of SiNWs is more sensitive to the coverage of colloidal patterns than the NW density. SEM observations revealed that thin Si layers were unintentionally grown on the catalytically patterned areas, whereas no Si layer was formed on the bare substrate surfaces. A theoretical study predicted that a Si thin film has much higher reflectivity than SiNWs, and therefore we can conclude that the enhanced optical transmittance with a decrease in the coverage of colloidal patterns might be due to the reduced reflection by the unintentionally grown Si thin films. These optical characterizations also suggest that the transmittance of SiNWs can be controlled by varying the catalytic pattern size and/or the line spacing.

Conclusions

We have presented the patterned synthesis of SiNWs on glass substrates using a colloid-catalyzed CVD method,

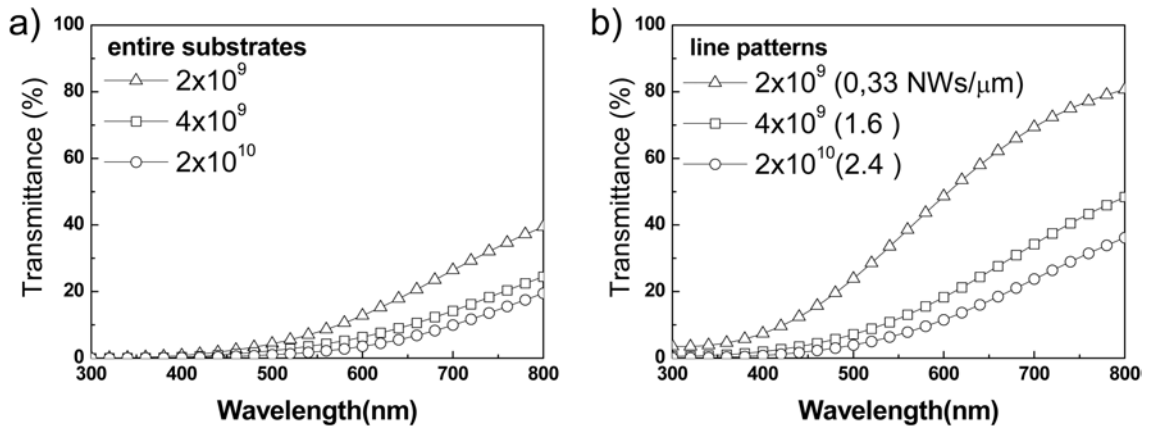


Fig. 4. (a) Optical transmittance spectra of SiNWs grown on the colloid deposited glass substrates prepared with different concentrations of colloidal Au solutions, (b) Optical transmittance spectra of SiNWs selectively grown on the line patterns of the Au colloid with 40 μm line/spacing prepared with different concentrations of colloidal Au solutions.

combined with a colloid patterning technique. Au colloid patterns with variable shape, size, and particle density serve as favorable sites for the initiation of SiNW growth, leading to selective and lateral growth of SiNWs, useful for device integration. In addition, optical characterization revealed that SiNW pattern arrays are quite transparent in the long wavelength spectral region (700-800 nm) with a transmittance of ~70-80%, whereas the transmittance is significantly affected by the coverage of colloidal patterns prepared for SiNW growth.

Acknowledgements

This research was supported by Hanyang Fusion Materials Program funded by Ministry of Education, Science and Technology, Korea.

References

1. R.H. Reuss, D.G Hopper and J.-G Park, MRS Bull. 31[6] (2006) 447-454.
2. Y. Sun, S.-H. Hur and J.A. Rogers, in "Springer Handbook of Nanotechnology" (Springer, 2007) 375-398.
3. E. Menard, K.J. Lee, D.-Y. Khang, R.G. Nuzzo and J.A. Rogers, Appl. Phys. Lett. 84[26] (2004) 5398-5400.
4. X. Duan, C. Niu, V. Sahi, J. Chen, J.W. Parce, S. Empedocles and J.L. Goldman, Nature 425[6955] (2003) 274-278.
5. R.S. Friedman, M.C. McAlpine, D.S. Ricketts, D. Ham and C.M. Lieber, Nature 434[7037] (2005) 1085.
6. H.-M. Kim, T.W. Kang and K.S. Chung, J. Ceram. Process. Res. 5[3] (2004) 241-243
7. L. Hu and G. Chen, Nano lett. 7[11] (2007) 3249-3252.
8. B. Tian, X. Zheng, T.J. Kempa, Y. Fang, N. Yu, G. Yu, J. Huang and C. M. Lieber, Nature 449[7164] (2007) 885-889.
9. L. Tsakalakos, J. Balch, J. Fronheiser, B. A. Korevaar, O. Sulima and J. Rand, Appl. Phys. Lett. 91[23] (2007) 117-233.
10. S. Ju, A. Facchetti, Y. Xuan, J. Liu, F. Ishikawa, P. Ye, C. Zhou, T.J. Marks and D.B. Janes, Nat. Nanotech. 2[6] (2007) 378-384.
11. E.N. Dattoli, Q. Wan, W. Guo, Y. Chen, X. Pan and Wei Lu, Nano Lett. 7[8] (2007) 2463-2469.
12. E. Artukovic, M. Kaempgen, D. Hecht, S. Roth and G. Grüner, Nano Lett. 5[4] (2005) 757-760.
13. Q. Cao, S.-H. Hur, Z.-T. Zhu, Y. Sun, C. Wang, M. Meitl, M. Shim and J. A. Rogers, Adv. Mater. 18[3] (2006) 304-309.
14. A.I. Hochbaum, R. Fan, R. He and P. Yang, Nano Lett. 5[3] (2005) 457-460.
15. R. He, D. Gao, R. Fan, A.I. Hochbaum, C. Carraro, R. Maboudian, and P. Yang, Adv. Mater. 17[17] (2005) 2098-2102.
16. Y. Cui, L.J. Lauhon, M.S. Gudiksen, J. Wang and C.M. Lieber, Appl. Phys. Lett. 78[15] (2001) 2214-2216.
17. F. Patolsky, G. Zheng and C. M. Lieber, Nat. Protoc. 1[4] (2006) 1711-1724.
18. R.S. Wagner and W.C. Ellis, Appl. Phys. Lett. 4[5] (1964) 89-90.
19. Y. Wu and P. Yang, J. Am. Chem. Soc. 123[13] (2001) 3165-3166.
20. J. Kong, H.T. Soh, A. Cassell, C.F. Quate and H. Dai, Nature 395[6705] (1998) 878-880.